JOC The Journal of Organic Chemistry

Article

pubs.acs.org/joc

# Bridged Tolanes: A Twisted Tale

Sebastian Menning,[†] Maximilian Krämer,[‡] Andrew Duckworth,[§] Frank Rominger,[†] Andrew Beeby,[§,*] Andreas Dreuw,[‡,∥,*] and Uwe H. F. Bunz[†,∥,*]

[†]Organisch-Chemisches Institut, Ruprecht-Karls-Universität Heidelberg, Im Neuenheimer Feld 270, 69120 Heidelberg, Germany

[‡]Interdisziplinäres Zentrum für Wissenschaftliches Rechnen (IWR), Ruprecht-Karls-Universität Heidelberg, Im Neuenheimer Feld 368, 69120 Heidelberg, Germany

[§]Department of Chemistry, Durham University, South Road, Durham DH 3LE, U.K.

[∥]Centre for Advanced Materials (CAM), Im Neuenheimer Feld 225, 69120 Heidelberg, Germany

Supporting Information

**ABSTRACT:** The rotational motion of tolanes along their acetylene axis is not fully understood. What happens to the optical and electronic properties if the tolane backbone is forced into a twisted conformation? Several tethers were investigated to obtain tolanophanes, fixing the torsion angle of the two phenyl rings. X-ray crystal structures revealed tether-specific torsion angles in the solid state. The absorption, emission, and excitation spectra were recorded. Twisted tethered tolane conformers showed blue-shifted absorption; emission spectra were all torsionally independent and identical. The tethered tolanes were embedded in a rigid matrix by freezing to 77 K; well-resolved emission spectra were recorded for planar tolanes, but for twisted systems unexpectedly long-lived phosphorescence was observed. How is this triplet emission explained? Quantum chemical calculations (TDDFT/cam-B3LYP/6-31G*) of the unsubstituted tolane showed that intersystem crossing (ISC) is favored with large spin−orbit coupling, which occurs when the molecular orbitals are orthogonal to each other; this is the case at the crossing of $S_1/T_7$. Also, a small energy difference between singlet and triplet states is required; we found that ISC can favorably take place at four crossings: $S_1/T_6$, $S_1/T_7$, $S_1/T_{8,9}$, $S_1/T_{10}$.

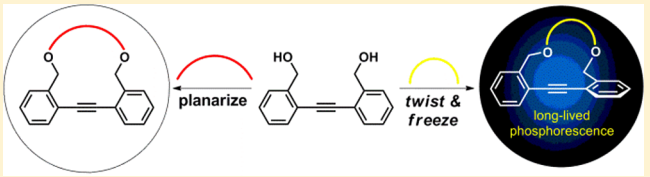


## INTRODUCTION

Tolane (diphenylacetylene) is a fundamental building block for conjugated organic oligomers, polymers and dendrimers.[1−4] The tolane framework is conformationally rigid, except for its single degree of freedom, the rotation around the acetylene axis, featuring a barrier of 2.4 kJ/mol.[5] Influencing the rotational motion of these linear chromophores is a significant tool to influence their photophysical properties.[6−13]

If the torsion angle $\alpha$ between the two aromatic rings switches from a planar to an orthogonal geometry, conjugation of the system will reduce. This decrease of electronic communication is illustrated by the position of the HOMO (highest occupied molecular orbital) and LUMO (lowest unoccupied molecular orbital) energies. The higher HOMO−LUMO gap in a fully twisted tolane leads to the observed hypsochromic shift in absorption.[9,14,15] Standard quantum chemical calculations paint this simplified picture (see Supporting Information).

The photophysical behavior of tolane is peculiar. In its ground state, tolane has $D_{2h}$ symmetry. Excitation to the linear $1^1B_{1u}$ ($\pi\pi^*$) state (lifetime $\tau$ = 8 ps) is followed by internal conversion (IC) to the trans-bent $1^1A_u$ ($\pi\sigma^*$) "dark" state ($\tau$ = 200 ps) with $C_{2h}$ symmetry (Figure 1).[16−18] The two $\pi$-orbitals of the C−C triple bond enhance the spin−orbit coupling, which is responsible for an intersystem crossing (ISC), resulting in the triplet state $T_1$.[19] The main fluorescence arises from $1^1B_{1u} \rightarrow 1^1A_g$. Emission from the "dark" state ($1^1A_u \rightarrow 1^1A_g$) is weak due to its bent, stilbene-like structure.[20] The triplet state ($1^3B_{1u}$) is linear with a lifetime of $\tau$ = 1 $\mu$s.[21−23]

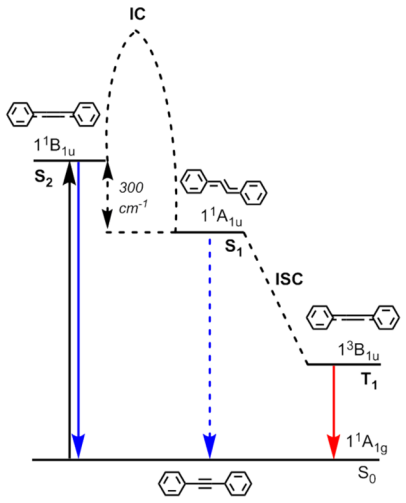


**Figure 1.** Simplified illustration of low-lying excited states of tolane.

**Received:** May 11, 2014
**Published:** June 17, 2014

   dx.doi.org/10.1021/jo5010235 | J. Org. Chem. 2014, 79, 6571−6578

Tolanes twist either through sterically demanding groups[15,24−32] or by choosing a suitable tether, connecting the two phenyl rings. Yang et al. used pentiptycene groups to impart steric bulk into the tolane system and prepared a series of tolane oligomers. Because of their twisted conformation both a blue-shift in absorption and emission was observed at 80 K.

For tolanophanes, different tethers were investigated, but up to now the highest torsion angle in the solid state was 34°.[14,33,34] In 2013 we reported a vertically twisted tolane, phosphorescing brightly at 77 K. In this contribution we expand synthetic access to further tethered tolanes and explore their photophysics. All of the twisted systems show a fascinating long-lived triplet emission while planar tolanes fluoresce.[35]

## RESULTS AND DISCUSSION

**Syntheses.** The tolanophanes **2**, **4**−**10** were prepared in a two-step reaction. Diol **1**,[36,37] made by Sonogashira reaction of 2-iodobenzyl alcohol with acetylene gas, was transformed into the tolanophanes **2** and **4**−**10** by reaction with diacid chlorides in the presence of an auxiliary base under high dilution conditions (Scheme 1). To influence the torsion angle of **2**, the

**Scheme 1. Syntheses of Bridged Tolanes (X = Tether)**

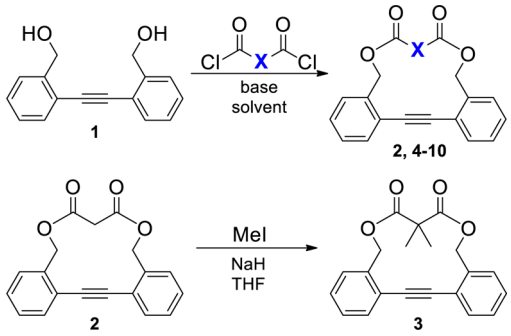


malonyl-tether in **2** was dimethylated in the $\alpha$-position furnishing **3** in 56% yield. As a structurally flexible tether, succinyl was inserted, resulting in the flexible ring system **4**. Stiffening the tether of this system was achieved by the syntheses of the tolanophanes **5**−**10** (Table 1). The tethered tolanes were obtained after aqueous workup followed by chromatographic purification. Yields vary from 6 to 35% in this ring closure reaction.

**Ground State Conformations.** We obtained single crystalline specimen from compounds **1**−**9** using different solvent mixtures (see Supporting Information),[38] and colorless needles of **2**−**9** were analyzed by X-ray crystallography. For tolane **10** repeated attempts of crystallization failed due to its low solubility. Because of ring strain, tolane axes have little deviation from linearity (<9°). The strapped systems show different torsion angles depending on the tether we used (Figure 2).[39]

For tolanes **2**, **4**, **6** and **9** torsions angles around 80° resulted. **2** was methylated into **3** to see if the torsion angle would change. We found two molecules in the unit cell of **3** with $\alpha_1$ = 69° and $\alpha_2$ = 80°. Surprisingly, compound **4** with the softer succinyl bridge shows maximum twist, at least in the solid state. Tolanophanes **6** and **9**, where the tether is stiffer, twist by 75 and 72°. An almost planar conformation is observed for **5**, **7** and **8**.

We computed all possible ground state conformations of all investigated tolanes **2**−**10** at the theoretical level of DFT-D3/B3LYP/cc-pVTZ (Table 2).[40−42] Most tolanes have several ground state conformers, which span a range of torsion angles. For example tolanes **2** and **3** possess a twisted global minimum with a twist angle of 72° that is about 10 kJ/mol lower in energy than two almost planar isomers. However, dependent on the tether of the different tolanes, the relative energies of planar and twisted isomers change and, as a consequence, their Boltzmann distribution at thermal equilibrium. While the tolanes **2**, **3**, **6**, **9** and **10** prefer twisted conformations with Boltzmann populations of the corresponding minima with

**Table 1. Reaction Conditions for Syntheses of Bridged Tolanes**

| Tolane | Tether X | Reaction Conditions | Yield, % |
|---|---|---|---|
| **2** |  | malonyl chloride $NaHCO_3$, DCM | 35 |
| **3** |  | methyl iodide, NaH THF | 56 |
| **4** |  | succinyl chloride $NaHCO_3$, DCM | 20 |
| **5** |  | *trans*-1,2-cyclohexane-dicarbonyl chloride $NaHCO_3$, DCM | 32 |
| **6** |  | fumaryl chloride DMAP, $NEt_3$, DCM | 10 |
| **7** |  | bicyclo[2.2.1]hepta-2,5-diene-2,3-dicarbonyl chloride DMAP, $NEt_3$, DCM | 7 |
| **8** |  | phthaloyl chloride $NEt_3$, THF | 18 |
| **9** | 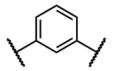 | isophthaloyl chloride $NEt_3$, THF | 33 |
| **10** | 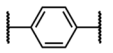 | terephthaloyl chloride $NEt_3$, THF | 6 |

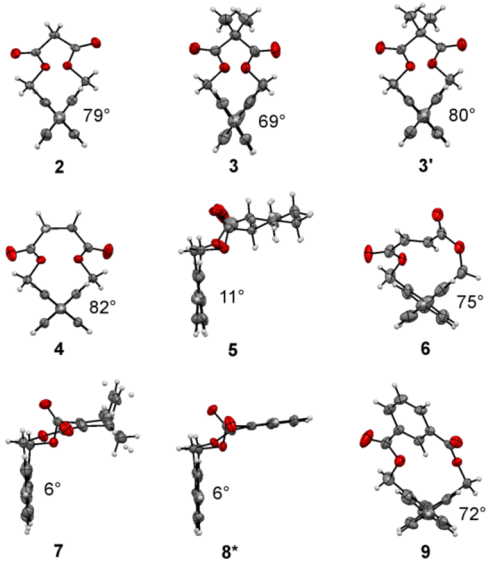


**Figure 2.** Crystal structures and torsion angles of **2**−**9**. *Two independent molecules were found in the unit cell. Both had planar conformation with torsion angles of $\alpha_1$ = 4°; $\alpha_2$ = 6°. Here we show the conformer with the torsion angle $\alpha_2$ due to similarity.


dx.doi.org/10.1021/jo5010235 | J. Org. Chem. 2014, 79, 6571−6578

**Table 2. Overview of the Tolanes 2−10 with the According Torsion Angle and Their Boltzmann Population at the Theoretical Level of DFT-D3/B3LYP/cc-pVTZ**

| tolane | torsion angle $\alpha$, crystal [deg] | torsion angle $\alpha$, calculated [deg] | Boltzman ensemble [%] | relative energy [kJ/mol] |
|---|---|---|---|---|
| **2** | 79 | 72 | 94.4 | 0 |
| | | 18 | 4.1 | 7.8 |
| | | 86 | 1.5 | 10.2 |
| **3** | 69, 80 | 72 | 97.1 | 0.0 |
| | | 20 | 2.1 | 9.5 |
| | | 85 | 0.8 | 11.9 |
| **4** | 82 | 79 | 48.5 | 0.0 |
| | | 6 | 22.9 | 1.9 |
| | | 77 | 17.2 | 2.6 |
| | | 73 | 5.8 | 5.3 |
| | | 29 | 5.6 | 5.4 |
| **5** | 11 | 6 | 80.7 | 0.0 |
| | | 88 | 18.0 | 3.7 |
| | | 4 | 1.0 | 11.0 |
| | | 77 | 0.2 | 15.6 |
| | | 83 | 0.1 | 18.3 |
| **6** | 75 | 80 | 99.5 | 0.0 |
| | | 83 | 0.4 | 13.7 |
| | | 66 | 0.1 | 18.6 |
| **7** | 6 | 11 | 60.1 | 0.0 |
| | | 80 | 19.3 | 2.8 |
| | | 87 | 17.8 | 3.0 |
| | | 12 | 2.8 | 7.6 |
| **8** | 4, 6 | 9 | 95.4 | 0.0 |
| | | 80 | 4.6 | 7.5 |
| **9** | 72 | 67 | 99.9 | 0.0 |
| **10** | – | 50 | 76.6 | 0.0 |
| | | 56 | 20.8 | 3.2 |
| | | 60 | 2.7 | 8.3 |

more than 80%, the tolanes **5**, **7** and **8** exhibit preferentially planar ground state structures. The only exception is tolane **4**, which, because of its flexible tether, can adopt planar as well as twisted conformations at room temperature.

Considering all the tethered systems, a simple prediction of the twist angle depending on the molecular structure is not possible. Synthesis followed by X-ray analysis or a priori quantum chemical calculations are necessary. But how does the variation of the twist angle $\alpha$ influences their photophysical behavior, or does it not at all?

**Excited State Conformations.** For all the targets absorption, excitation and emission spectra were recorded in *n*-hexane at room temperature. Figure 3a shows the absorption spectra of the planar systems (**5**, **7** and **8**) with their main maxima at 310 nm. The twisted derivatives **2**–**4**, **6**, **9** (and **10**) experience a hypsochromic shift in their UV−vis spectra (Figure 3b); decreased conjugation results in a higher HOMO−LUMO gap. As an exception, tolanes **4** and **10** should be focused on. The shape of the absorbance shows a similarity to the planar derivatives, despite the almost perpendicular geometry of **4** in the crystal structure. This could be explained by the flexible (**4**) and long (**10**) tethers allowing facile planarization in solution. The excitation spectra show the relative emission intensity at 360 nm and reflect the absorption spectra (see Supporting Information). While the UV−vis spectra represent the torsion angle quite adequately, the shape of the emission spectra *is identical, regardless of twisting* (Figure 3c). In solution planarization of the excited state is apparently fast, so that emission does not occur from the twisted species.[43]

Neither extinction coefficients nor fluorescence quantum yields are dependent on the twist angle (Table 3). The "open" tolane **1** has an absorption coefficient of $2 \times 10^4$ L mol$^{-1}$ cm$^{-1}$, while planar **8**, with the stiffest tether of all the planar derivatives, shows an absorptivity of $3 \times 10^4$ L mol$^{-1}$ cm$^{-1}$. For twisted tolanes **2**–**4**, **6**, **9** (and **10**) the coefficients range from $1-1.5 \times 10^4$ L mol$^{-1}$ cm$^{-1}$. The quantum yields were measured in two solvents, *n*-hexane and dichloromethane, and are lower in the more polar solvent, as expected. Torsion angle and quantum yield are apparently independent, and for all tolanes the fluorescence lifetimes were short (~400 ps). From the steady state measurements we can glean that some tethered tolanes show a twisted ground state conformation in solution as suggested by X-ray crystallography and quantum chemical calculations. Considering the excited states, however, they all behave identically and emit from a planar conformation.

**Low Temperature Spectroscopy.** At room temperature all bridged tolanes show the same fluorescence spectra; they are all in a planar excited state conformation (Figure 3c).[43] To trap the ground state conformations and preserve them in the excited state, we dissolved the tolanophanes in EPA (mixture of diethyl ether/isopentane/ethanol 5:5:2), a transparent organic glass at 77 K.

Freezing the compounds to 77 K, we "lock in" the ground state conformation and assume that the structure in the glass is similar to that observed in the crystalline state. Figure 4 shows the spectra at room temperature (top, red) and at 77 K (bottom, blue) of the two twisted systems **3**, **4** and the planar derivative **5**. Spectra of other tethered tolanes are not shown but similar (see Supporting Information). Both absorption and

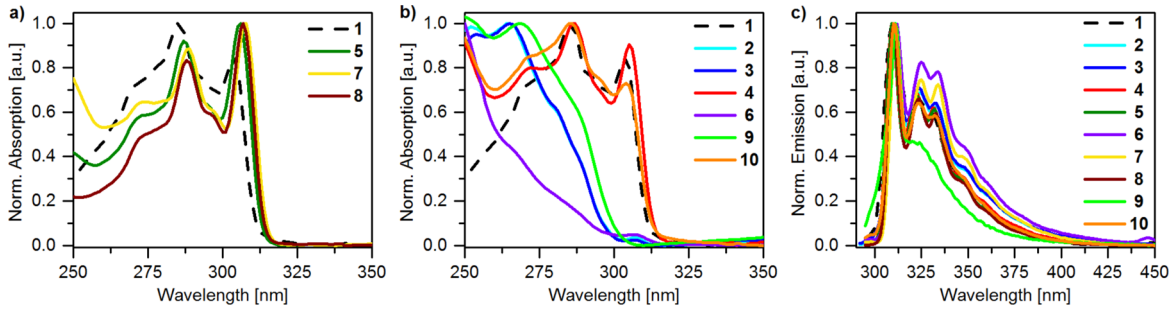


**Figure 3.** Absorption spectra of (a) planar and (b) twisted conformers. (c) Emission spectra of compounds **1**−**10**. All spectra in *n*-hexane at room temperature.


dx.doi.org/10.1021/jo5010235 | J. Org. Chem. 2014, 79, 6571−6578

**Table 3. Photophysical Properties of Tolanes 1−10**

| tolane | torsion angle $\alpha$ [deg] | $\lambda_{max}{}^{b}$ [nm] absorption | $\varepsilon^{c}$ [$10^4$ L mol$^{-1}$ cm$^{-1}$] | $\lambda_{max}{}^{b}$ [nm] emission | $\Phi^{b}$ [%] | $\Phi^{c}$ [%] | $\tau^{1}{}_{298K}{}^{b}$ [ps] | $\tau^{2}{}_{298K}{}^{b}$ [ps] | $\tau{}_{77K}{}^{d}$ [s] |
|---|---|---|---|---|---|---|---|---|---|
| **1** | 71 | 285 | 2.0 | 310 | 5.1 | 1.0 | 420 | 115 | – |
| **2** | 79 | 265 | 1.3 | 311 | 22.9 | 7.1 | 424 | 108 | 1.4 |
| **3** | 69, 80 | 265 | 1.3 | 311 | 15.5 | 4.7 | 430 | 175 | 1.4 |
| **4** | 82 | 286 | 1.3 | 309 | 21.9 | 10.8 | 437 | 54 | 1.1 |
| **5** | 11 | 306 | 1.9 | 309 | 27.8 | 33.9 | 460 | 3 | – |
| **6** | 75 | 285[a] | 0.6 | 311 | 4.1 | 0.2 | –[e] | –[e] | 0.8 |
| **7** | 6 | 308 | 1.3 | 311 | 2.2 | 0.2 | 446 | 31 | – |
| **8** | 4, 6 | 307 | 3.0 | 310 | 25.5 | 4.8 | 424 | 78 | – |
| **9** | 72 | 269 | 1.6 | 311 | 0.4 | 0.2 | –[e] | –[e] | 1.6 |
| **10** | – | 286 | 1.5 | 310 | 4.5 | 0.1 | 438 | 67 | 1.1 |

[a]Shoulder. [b]In *n*-hexane. [c]In dichloromethane. [d]In diethyl ether/isopentane/ethanol 5:5:2 (EPA). [e]Lack of appreciable fluorescence to detect signal.

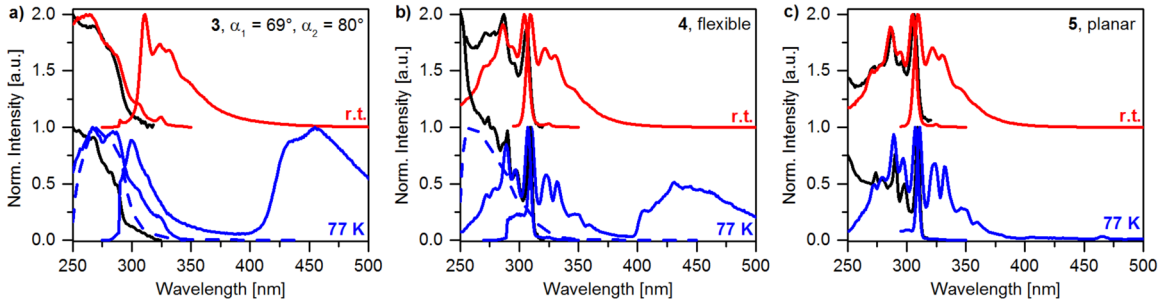


**Figure 4.** Absorption, excitation and emission spectra in EPA of the twisted conformers **3** (a) and **4** (b) and the planar species **5** (c). Black: Absorption at rt (top) and 77 K (bottom). Red: Excitation ($\lambda_{em}$ = 360 nm) and emission at rt. Blue: Excitation ($\lambda_{em}$ = 360 nm) and emission at 77 K. Blue dotted: Excitation ($\lambda_{em}$ = 460 nm) at 77 K. Torsion angles from the X-ray crystal structure.

emission spectra of the planar phanes (**5**, **7**, **8**) are well resolved.

The anticipated fluorescence blue-shift, when going from room temperature to 77 K, was observed for the twisted derivatives **2**, **3**, **9** (and **10**). For **4**, **6** and the planar tolanes **5**, **7**, **8** (and **1**) no hypsochromic shift was recorded. Additionally, for all twisted conformers strong phosphorescence around 450 nm was measured, and for **10** as well, which is why we reason it to be twisted.

It is noteworthy that excitation at different wavelengths ($\lambda_{ex}$ = 260−300 nm, 10 nm-steps, see Supporting Information) gave varying emission spectra with respect to the ratio of fluorescence/phosphorescence intensities. This occurs from different existing conformers. Exciting at 260 nm the twisted specimen emits and gives a strong phosphorescence signal, while the planar isomer gets excited at 300 nm recording only fluorescence. This could as well be seen in the excitation spectra, which detected the phosphorescence ($\lambda_{em}$ = 460 nm), showing the maximum at 260−270 nm (Figure 4, blue dotted line). These effects are observed in analogy to literature observations.[9]

In rigid systems triplets have a chance to phosphoresce as radiationless decay is less prevalent. The lifetime of the triplet state for unsubstituted tolane is 1 $\mu$s.[21] Measuring the phosphorescence lifetime of the twisted representatives **2**−**4**, **6**, **9** (and **10**), however, gives values around 1 s (Table 3). Figure 5 illustrates the fast decay of the fluorescence (280−380 nm) and the very slow disappearance of the phosphorescence signal (400−700 nm) of compound **2**. Such long-lived phosphorescence is new for tolanes and remarkable.

**Quantum Chemical Calculations.** Our and other researchers' experiments show that the torsion angle between the phenyl rings of tolanes determines the shape of their

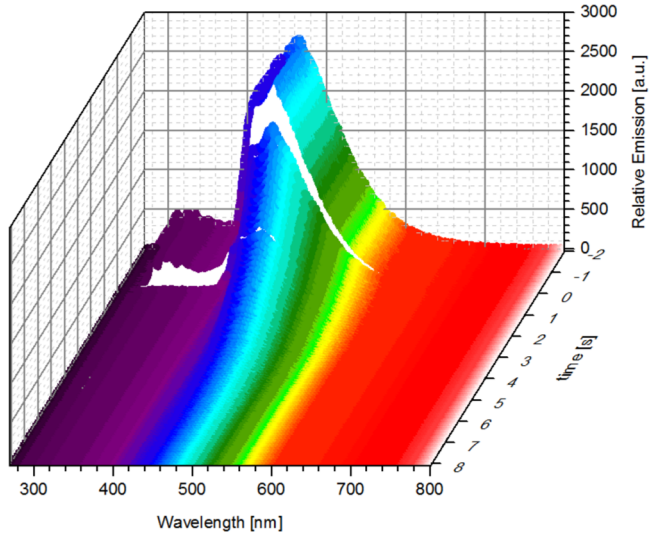


**Figure 5.** 3D illustration of luminescent decay of tolane **2**.

absorption profile.[9,14,15] In addition (vide supra) the torsion angle also influences the occurrence of phosphorescence at low temperatures. To gain insight into the photophysics of tolanes in general, a first important step is a detailed understanding of the photophysics of the unsubstituted parent tolane. Toward that objective, the vertical excited singlet and triplet states of tolane were computed along the twisting coordinate at the theoretical level of TDDFT/CAM B3LYP/6-31G*.[44−47]

At the planar geometry, the two lowest lying and thus relevant transitions $S_1$ and $S_2$ exhibit excitation energies of 4.7 and 5.2 eV and oscillator strengths of 1.1 and 0.0 respectively. In the molecular orbital picture the $S_1$ state is represented by a HOMO to LUMO transition. The $S_2$ state corresponds mainly


dx.doi.org/10.1021/jo5010235 | J. Org. Chem. 2014, 79, 6571−6578

to an electronic transition from the HOMO−4 (!) to the LUMO. HOMO and HOMO−4 reflect the orthogonal $\pi$-bonds of the central triple bond. At the fully twisted configuration, i.e., a torsion angle of 90°, the energy of the $S_1$ and $S_2$ states are interchanged possessing excitation energies of 5.2 and 5.1 eV, respectively (Figure 6). The HOMO to LUMO transition loses its oscillator strength continuously along the twisting coordinate until both states have no oscillator strength any more at 90°. At this geometry, the lowest excited state with substantial oscillator strength of 1.5 is $S_6$ at an excitation energy of 5.9 eV. This explains the strongly blue-shifted absorption spectra of twisted tolanes in contrast to planar ones.

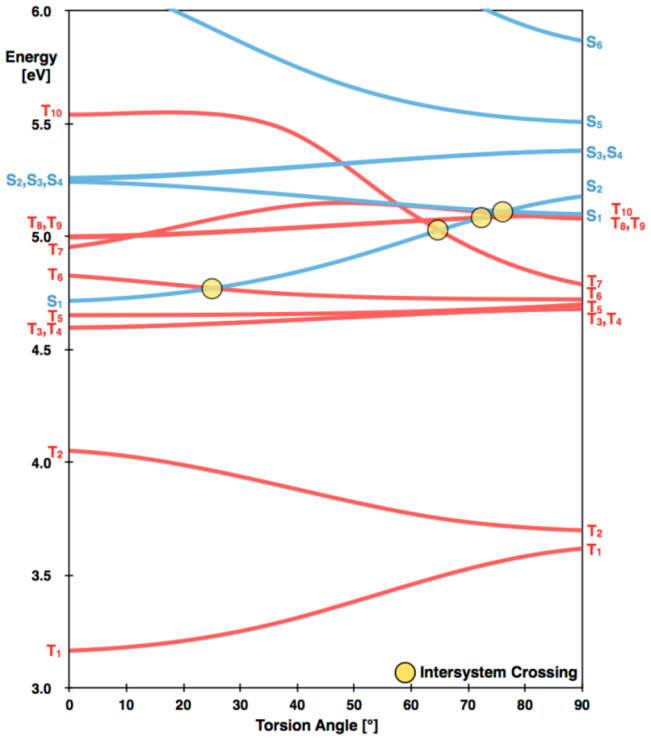


**Figure 6.** Potential energy curves of the lowest lying singlet (blue) and triplet (red) excited states of tolane along the twisting coordinate of the two phenyl rings. The curves were computed at the theoretical level of TDDFT/CAM B3LYP/6-31G*. The circles highlight relevant crossings between the lowest singlet and triplet states.

Inspection of the potential energy curves in Figure 6 reveals that the allowed HOMO−LUMO excitation always leads to a planarization of the tolanes. The global planar minimum on the $S_1$ surface of tolane lies at 0°, and from all other angles a barrierless transition into this minimum is possible in $S_1$. This nicely explains why planar and twisted tolanes exhibit different UV−vis absorption spectra, but why the fluorescence spectra are all equivalent and correspond to those of planar tolanes.

To further understand why twisted tolanes exhibit phosphorescence at low temperatures, while planar ones do not show this feature, the excited singlet and triplet states are considered. For phosphorescence to occur, intersystem crossing (ISC) must happen, which is facilitated by two requirements: large spin−orbit couplings and a small S-T energy difference. Upon initial excitation, the $S_1$ state is populated, and we assume that ISC occurs from this state. Following the $S_1$ curve of tolane along the twisting coordinate from 0° to 90° (Figure 6), four curve crossings with triplet states are identified: $S_1/T_6$ at 25°, $S_1/T_7$ at 65°, $S_1/T_{8/9}$ at 70° and $S_1/T_{10}$ at 75°, where ISC can favorably occur. However, large spin−orbit coupling is also required for efficient ISC, and to estimate its magnitude, El Sayed rules can be invoked.[48] According to these rules, spin−orbit coupling is particularly large when the molecular orbitals involved in the crossing of electronic singlet and triplet states are perpendicular to each other. Inspection of the molecular orbitals involved in these states reveals that the most likely place for ISC to occur is at the crossing between $S_1$ and $T_7$ at a torsion angle of 65°, since only for this pair of states, the orbitals are perpendicular to each other. Hence, at the theoretical level of TDDFT/CAM B3LYP/6-31G*, the most likely crossing for ISC to take place is between $S_1$ and $T_7$ (Figure 7).

This finding explains why only twisted tolanes exhibit phosphorescence at low temperatures. A tolane with small torsion angle is initially excited into the $S_1$ state, and ISC is very slow, because tolanes tend to planarize in the $S_1$ state, and the initial excitation is not high enough to reach the state crossing with $T_7$ at 65° torsion. The situation is different when a twisted tolane is excited in a frozen matrix. Then the initial excitation energy lies higher than the state crossing, and moreover, the induced planarization of the tolane leads barrierless to the $S_1/T_7$ crossing where most likely ISC can take place. Eventually,

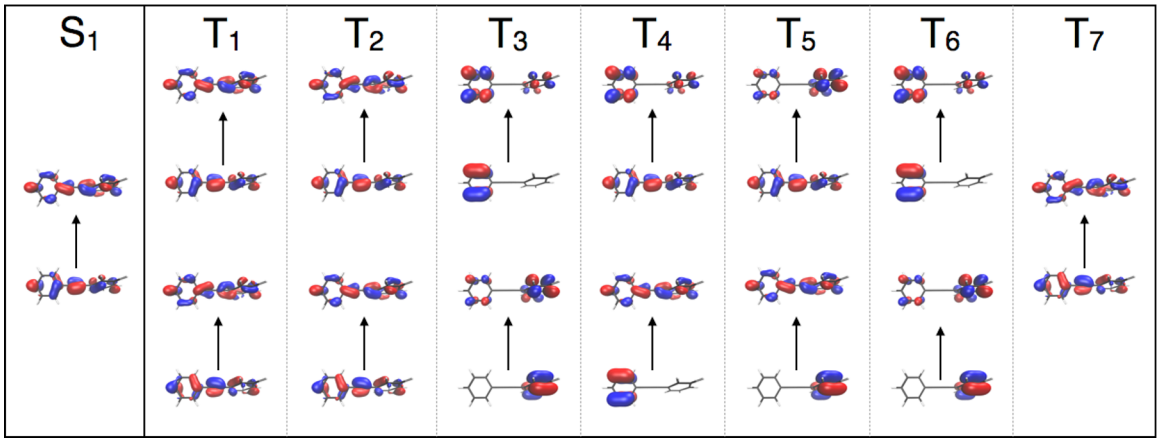


**Figure 7.** Molecular orbitals involved in lowest singlet state $S_1$ and in the energetically accessible triplet states $T_1$ to $T_7$ computed at the level of TDDFT/CAM B3LYP/6-31G*.


dx.doi.org/10.1021/jo5010235 | J. Org. Chem. 2014, 79, 6571−6578

the molecules decay nonradiatively into the $T_1$ minimum at 0° and phosphoresce strongly red-shifted. In agreement with the experimental findings, only tolanes with large arrested torsion angles can exhibit efficient phosphorescence.

**Tethered Tolanes.** The experimental findings agree perfectly to the calculated results. Compounds **5**, **7** and **8** are planar and nonphosphorescent and exhibit exclusively fluorescence at low temperature. In contrast, the twisted tolanes **2**, **3**, **6**, **9** and **10** show predominantly phosphorescence. Tolane **4** is an intermediate case as it shows both strong fluorescence and phosphorescence at low temperature in agreement with the calculated population of planar as well as twisted ground state minima.

## CONCLUSION

We have prepared a series of tolanophanes with torsion angles that can be "dialed in", depending upon the chemical nature of the bridging group. Twisting of the tolanes is documented by crystal structures, DFT-calculations and optical (absorption) spectroscopy. As the absorption spectra blue-shift in dependence of the torsion angle, i.e., twisting diminishes the conjugation, the emission is torsion angle independent, when measured in solution. Emission spectra of twisted tolanes recorded in organic glasses at cryogenic temperatures show efficient phosphorescence with emissive lifetimes of ca. 1 s. Quantum chemical calculations show that the $S_1$ intersects with the $T_7$-state and ISC is facile. Relaxation to $T_1$ is followed by phosphorescence. Over all, twisting tolanes leads to surprising and exciting changes in their optical and electronic properties. The most unusual feature is their long-lived strong phosphorescence observed in cryogenic matrices.

## EXPERIMENTAL SECTION

**Materials and Methods.** Reactions were carried out in oven-dried glassware under an atmosphere of nitrogen using the common Schlenk-technique. For thin layer chromatography (TLC) silica gel plates were used and examined under ultraviolet light irradiation (254 and 365 nm). Column chromatography was performed using silica gel (particle size: 0.04−0.063 mm). All NMR spectra ($^1H$,$^{13}C$) were recorded at room temperature at 300 or 500 MHz in deuterated chloroform ($CDCl_3$). The chemical shifts ($\delta$) were reported in parts per million (ppm) and referenced internally to the solvent signal.[49] The following abbreviations were used in the listings of the NMR resonances: s (singlet), d (doublet), t (triplet), m (multiplet). For high resolution mass spectra (HRMS) the samples were ionized by electron impact (EI) in the positive mode and analyzed by magnetic sector. Solvents were abbreviated as PE (petroleum ether), EA (ethyl acetate), EtOH (ethanol).

**General Procedure (GP).** Simultaneous, dropwise addition of a solution of diol **1** and a second solution of the corresponding dichloride to base ($NaHCO_3$ or $NEt_3$, DMAP) in solvent (DCM or THF) was followed by stirring for 10 h at room temperature. In case of using DCM as solvent the organic phase was washed with water, brine, dried over $MgSO_4$ and evaporated under reduced pressure. If THF was used as solvent the mixture was concentrated in vacuo, and the residue was dissolved in DCM followed by aqueous workup as described above. After chromatographic purification (PE/EA 4:1) the desired tolanophane was obtained.

**Tolane 1.** 2,2′-(1,2-Ethynediyl)bis-benzenemethanol was synthesized by known procedure, see reference.[36,37]

**Tolane 2. GP.** The DCM-solutions (75 mL each) of **1** (600 mg, 2.52 mmol, 1.0 equiv) and malonyl chloride (0.3 mL, 2.77 mmol, 1.1 equiv) were added to a suspension of $NaHCO_3$ (635 mg, 7.55 mmol, 3.0 equiv) in DCM (200 mL) over a period of 4 h. After the described workup the crude product was subjected to chromatographic purification to provide tolane **2** (273 mg, 891 μmol, 35%) as a colorless solid: $R_f$ 0.43 (PE/EA 4:1); mp 232 °C; $^1H$ NMR (300 MHz) $\delta$ 3.40 (s, 2H), 5.16 (s, 4H), 7.35−7.43 (m, 6H), 7.56−7.59 (m, 2H); $^{13}C$ NMR (76 MHz) $\delta$ 42.0, 67.7, 90.8, 124.4, 128.9, 129.3, 130.7, 132.8, 136.4, 166.3; IR ($\nu$) 2954, 1751, 1724, 1495, 1462, 1405, 1377, 1297, 1276, 1210, 1151, 990, 760, 739; HRMS (EI) calcd for $M^+$ 306.0892, found 306.0884. Anal. Calcd for ($C_{19}H_{14}O_4$): C 74.50, H 4.61. Found: C 74.31, H 4.63.

**Tolane 3.** To a solution of tolane **2** (250 mg, 816 μmol, 1.0 equiv) in THF (10 mL) at 0 °C was added sodium hydride (58.8 mg, 2.45 mmol, 3.0 equiv). After stirring for 30 min methyl iodide (0.15 mL, 2.45 mmol, 3.0 equiv) was added, and the reaction mixture was stirred at room temperature for 48 h. The reaction mixture was quenched with ice−water (50 mL) and extracted with DCM (3 × 60 mL). The organic extract was washed with water (3 × 200 mL) and brine (150 mL), dried over $MgSO_4$ and concentrated in vacuo. After chromatographic purification tolane **3** (154 mg, 461 μmol, 56%) was obtained as a colorless solid: $R_f$ 0.64 (PE/EA 4:1); mp 182 °C; $^1H$ NMR (300 MHz) $\delta$ 1.43 (s, 6H), 5.09 (s, 4H), 7.34−7.42 (m, 6H), 7.54−7.57 (m, 2H); $^{13}C$ NMR (76 MHz) $\delta$ 22.8, 48.9, 67.7, 90.7, 124.5, 128.8, 129.2, 130.8, 132.5, 136.7, 173.1; IR ($\nu$) 2987, 1749, 1723, 1496, 1455, 1390, 1376, 1271, 1246, 1170, 1126, 929, 762, 751; HRMS (EI) calcd for $M^+$ 334.1205, found 334.1227.

**Tolane 4. GP.** To $NaHCO_3$ (1.06 g, 12.6 mmol, 5.0 equiv) in DCM (200 mL) were added **1** (600 mg, 2.52 mmol, 1.0 equiv) in DCM (75 mL) and succinyl chloride (0.3 mL, 2.77 mmol, 1.1 equiv) in DCM (75 mL) using two dropping funnels. Purification gave **4** (162 mg, 0.506 μmol, 20%) as a colorless solid: $R_f$ 0.39 (PE/EA 4:1); mp 195 °C; $^1H$ NMR (300 MHz) $\delta$ 2.63 (s, 4H), 5.22 (s, 4H), 7.33−7.41 (m, 4H), 7.44−7.47 (m, 2H), 7.59−7.62 (m, 2H); $^{13}C$ NMR (76 MHz) $\delta$ 30.1, 66.4, 91.2, 124.4, 128.8, 129.1, 131.2, 133.0, 136.9, 171.7; IR ($\nu$) 2956, 1722, 1495, 1462, 1417, 1377, 1336, 1229, 1165, 990, 976, 956, 879, 769; HRMS (EI) calcd for $M^+$ 320.1049, found 320.1050. Anal. Calcd for ($C_{20}H_{16}O_4$): C 74.99, H 5.03. Found: C 74.82, H 5.00.

**Tolane 5. GP.** Diol **1** (600 mg, 2.52 mmol, 1.0 equiv) in DCM (75 mL) and *trans*-1,2-cyclohexanedicarbonyl chloride[50,51] (579 mg, 2.77 mmol, 1.1 equiv) in DCM (75 mL) were added to $NaHCO_3$ (1.06 g, 12.6 mmol, 5.0 equiv) in DCM (150 mL) using two dropping funnels. After purification **5** (305 mg, 815 μmol, 32%) was isolated as a colorless solid: $R_f$ 0.60 (PE/EA 4:1); mp 255 °C; $^1H$ NMR (300 MHz) $\delta$ 1.17−1.39 (m, 4H), 1.75 (d, 2H, *J* 8.4 Hz), 2.06 (d, 2H, *J* 9.7 Hz), 2.55−2.65 (m, 2H), 5.03 (d, 2H, *J* 11.3 Hz), 5.35 (d, 2H, *J* 11.2 Hz), 7.24−7.34 (m, 4H), 7.44−7.47 (m, 2H), 7.60−7.63 (m, 2H); $^{13}C$ NMR (76 MHz) $\delta$ 25.2, 29.1, 45.2, 66.4, 91.5, 124.5, 128.8, 129.1, 131.3, 133.1, 136.9, 174.7; IR ($\nu$) 2937, 2861, 1722, 1495, 1446, 1389, 1372, 1316, 1256, 1220, 1170, 1112, 1002, 982, 757; HRMS (EI) calcd for $M^+$ 374.1518, found 374.1514. Anal. Calcd for ($C_{24}H_{22}O_4$): C 76.99, H 5.92. Found: C 76.85, H 5.89.

**Tolane 6.** According to reference:[52] To a solution of **1** (500 mg, 2.10 mmol, 1.0 equiv) in dry DCM (400 mL) were given $NEt_3$ (0.8 mL, 5.67 mmol, 2.7 equiv) and DMAP (0.128 g, 1.05 mmol, 0.5 equiv). Then fumaryl chloride (0.3 mL, 2.31 mmol, 1.1 equiv) was added slowly to the mixture, and the whole solution was stirred for 20 min. After washing with water (3 × 300 mL) and brine (300 mL) the organic layer was dried over $MgSO_4$ and concentrated in vacuo. After chromatographic purification and final recrystallization from EtOH **6** (67.7 mg, 0.213 mmol, 10%) was obtained as a colorless solid: $R_f$ 0.27 (PE/EA 4:1); mp 167 °C; $^1H$ NMR (300 MHz) $\delta$ 5.39 (s, 4H), 7.17 (s, 2H), 3.35−7.44 (m, 4H), 7.49−7.51 (m, 2H), 7.57−7.59 (m, 2H); $^{13}C$ NMR (126 MHz) $\delta$ 67.7, 91.2, 122.2, 129.1, 129.5, 130.3, 133.4, 133.5, 137.0, 165.2; IR ($\nu$) 2916, 1713, 1636, 1496, 1478, 1446, 1324, 1261, 1159, 1023, 987, 761; HRMS (EI) calcd for $M^+$ 318.0892, found 318.0877.

**Tolane 7.** Norborna-2,5-diene-2,3-dicarboxylic acid[53] (401 mg, 1.85 mmol, 1.1 equiv) was added slowly to a solution of **1** (400 mg, 1.68 mmol, 1.0 equiv), $NEt_3$ (0.63 mL, 4.53 mmol, 2.7 equiv) and DMAP (103 mg, 839 μmol, 0.5 equiv) in DCM (320 mL). After stirring with water the solution was washed with water (3 × 300 mL), brine (300 mL) and dried over $MgSO_4$. Concentration in vacuo and final chromatographic purification provided **7** (45.7 mg, 120 μmol,


dx.doi.org/10.1021/jo5010235 | J. Org. Chem. 2014, 79, 6571−6578

7%) as a colorless solid: $R_f$ 0.50 (PE/EA 4:1); mp 183 °C; $^1$H NMR (300 MHz) $\delta$ 2.01 (dt, 1H, $J$ 6.8, 1.4 Hz), 2.22 (dt, 1H, $J$ 6.8, 1.4 Hz), 3.90 (dt, 2H, $J$ 3.8, 1.6 Hz), 5.28 (s, 4H), 6.89 (t, 2H, $J$ 1.9 Hz), 7.33−7.42 (m, 4H), 7.45−7.48 (m, 2H), 7.58−7.61 (m, 2H); $^{13}$C NMR (76 MHz) $\delta$ 53.8, 67.2, 72.4. 91.8, 124.6, 128.8, 129.2, 131.4, 132.7, 136.7, 142.5, 151.0, 166.1; IR ($\nu$) 2981, 2942, 1718, 1704, 1557, 1489, 1380, 1258, 1084, 1049, 932, 753, 727; HRMS (EI) calcd for $M^+$ 382.1205, found 382.1191.

**Tolane 8.** According to **GP** the THF-solutions (25 mL each) of **1** (500 mg, 2.10 mmol, 1.0 equiv) and phthaloyl chloride (0.3 mL, 2.31 mmol, 1.1 equiv) were dropped into a mixture of $NEt_3$ (2.9 mL, 8.39 mmol, 10.0 equiv) and THF (300 mL). Following the workup as described above and chromatographic purification (PE/EA 4:1) tolane **8** (136 mg, 369 $\mu$mol, 18%) was obtained as a colorless solid: $R_f$ 0.43 (PE/EA 4:1); mp 243 °C; $^1$H NMR (300 MHz) $\delta$ 5.43 (s, 4H), 7.37−7.40 (m, 4H), 7.46 (td, 2H, $J$ 3.3, 2.9 Hz), 7.55−7.58 (m, 2H), 7.62−7.68 (m, 4H). $^{13}$C NMR (76 MHz) $\delta$ 67.9, 92.2, 124.6, 128.7, 128.7, 129.2, 131.0, 131.5, 131.9, 133.4, 136.2, 167.8; IR ($\nu$) 3061, 2952, 1716, 1602, 1496, 1450, 1373, 1276, 1249, 1119, 938, 757, 703, 693; HRMS (EI) calcd for $M^+$ 368.1049, found 368.1029. Anal. Calcd for ($C_{24}H_{16}O_4$): C 78.25, H 4.38. Found: C 77.87, H 4.56.

**Tolane 9. GP.** The THF-solutions (25 mL each) of **1** (500 mg, 2.10 mmol, 1.0 equiv) and isophthaloyl chloride (469 mg, 2.31 mmol, 1.1 equiv) were given to $NEt_3$ (2.9 mL, 8.39 mmol, 10.0 equiv) in THF (300 mL). Purification as described and column chromatography led to **9** (255 mg, 692 $\mu$mol, 33%) as a colorless solid: $R_f$ 0.46 (PE/EA 4:1); mp 208 °C; $^1$H NMR (300 MHz) $\delta$ 5.53 (s, 4H), 7.30−7.37 (m, 4H), 7.39−7.45 (m, 3H), 7.67−7.70 (m, 2H), 8.01 (dd, 2H, $J$ 7.7, 1.8 Hz), 9.77 (t, 1H, $J$ 1.7 Hz); $^{13}$C NMR (76 MHz) $\delta$ 66.2, 92.2, 123.8, 128.7, 128.8, 130.5, 131.5, 132.4, 135.2, 136.7, 137.0, 165.3; IR ($\nu$) 3137, 2952, 1719, 1491, 1448, 1428, 1368, 1287, 1126, 1060, 756, 719, 708; HRMS (EI) calcd for $M^+$ 368.1049, found 368.1078. Anal. Calcd for ($C_{24}H_{16}O_4$): C 78.25, H 4.38. Found: C 77.95, H 4.45.

**Tolane 10.** According to **GP**, a THF-solution of **1** (500 mg, 2.10 mmol, 1.0 equiv) in THF (25 mL) and a THF-solution (25 mL) of terephthaloyl chloride (469 mg, 2.31 mmol, 1.1 equiv) were added to $NEt_3$ (2.9 mL, 8.39 mmol, 10.0 equiv) in THF (300 mL). After usual workup and chromatographic purification tolane **10** (44.9 mg, 122 $\mu$mol, 6%) was obtained as a colorless solid (very low solubility): $R_f$ 0.40 (PE/EA 4:1); mp 250 °C; $^1$H NMR (300 MHz) $\delta$ 5.45 (s, 4H), 7.35−7.42 (m, 6H), 7.62−7.65 (m, 2H), 7.80 (s, 4H); $^{13}$C NMR (76 MHz) $\delta$ 65.9, 91.5, 123.1, 128.7, 129.0, 129.3, 129.6, 132.7, 133.6, 137.2, 165.3; IR ($\nu$) 3055, 2920, 1703, 1495, 1453, 1408, 1376, 1363, 1246, 1083, 1015, 927, 880, 748, 729; HRMS (EI) calcd for $M^+$ 368.1049, found 368.1027.

## ■ ASSOCIATED CONTENT

### Supporting Information

NMR spectra, X-ray crystal structures (CIF), photophysical data and quantum chemical calculation details. This material is available free of charge via the Internet at http://pubs.acs.org.

## ■ AUTHOR INFORMATION


### Corresponding Authors

*E-mail: andrew.beeby@durham.ac.uk.
*E-mail: dreuw@uni-heidelberg.de.
*E-mail: uwe.bunz@oci.uni-heidelberg.de.


### Notes

The authors declare no competing financial interest.

## ■ REFERENCES


(1) Bunz, U. H. F. *Chem. Rev.* **2000**, *100*, 1605.
(2) Bunz, U. H. F. In *Poly(Arylene Etynylene)S: From Synthesis to Application*; Weder, C., Ed.; Springer: Berlin, 2005; Vol. *177*, p 1.
(3) Zhang, W.; Moore, J. S. *Angew. Chem., Int. Ed.* **2006**, *45*, 4416.
(4) Moore, J. S. *Acc. Chem. Res.* **1997**, *30*, 402.
(5) Toyota, S. *Chem. Rev.* **2010**, *110*, 5398.
(6) Bunz, U. H. F. *Macromol. Rapid Commun.* **2009**, *30*, 772.
(7) Schmieder, K.; Levitus, M.; Dang, H.; Garcia-Garibay, M. A. *J. Phys. Chem. A* **2002**, *106*, 1551.
(8) Levitus, M.; Garcia-Garibay, M. A. *J. Phys. Chem. A* **2000**, *104*, 8632.
(9) Levitus, M.; Schmieder, K.; Ricks, H.; Shimizu, K. D.; Bunz, U. H. F.; Garcia-Garibay, M. A. *J. Am. Chem. Soc.* **2001**, *123*, 4259.
(10) Pesak, D. J.; Moore, J. S.; Wheat, T. E. *Macromolecules* **1997**, *30*, 6467.
(11) Melinger, J. S.; Pan, Y.; Kleiman, V. D.; Peng, Z.; Davis, B. L.; McMorrow, D.; Lu, M. *J. Am. Chem. Soc.* **2002**, *124*, 12002.
(12) Nakano, M.; Fujita, H.; Takahata, M.; Yamaguchi, K. *J. Am. Chem. Soc.* **2002**, *124*, 9648.
(13) Kim, J.; Swager, T. M. *Nature (London, U. K.)* **2001**, *411*, 1030.
(14) Brizius, G.; Billingsley, K.; Smith, M. D.; Bunz, U. H. F. *Org. Lett.* **2003**, *5*, 3951.
(15) Toyota, S.; Iida, T.; Kunizane, C.; Tanifuji, N.; Yoshida, Y. *Org. Biomol. Chem.* **2003**, *1*, 2298.
(16) Amatatsu, Y.; Hosokawa, M. *J. Phys. Chem. A* **2004**, *108*, 10238.
(17) Zgierski, M. Z.; Lim, E. C. *Chem. Phys. Lett.* **2004**, *387*, 352.
(18) Suzuki, T.; Nakamura, M.; Isozaki, T.; Ikoma, T. *Int. J. Thermophys.* **2012**, *33*, 2046.
(19) Hirata, Y.; Okada, T.; Mataga, N.; Nomoto, T. *J. Phys. Chem.* **1992**, *96*, 6559.
(20) Saltiel, J.; Kumar, V. K. R. *J. Phys. Chem. A* **2012**, *116*, 10548.
(21) Hiura, H.; Takahashi, H. *J. Phys. Chem.* **1992**, *96*, 8909.
(22) Nagano, Y.; Ikoma, T.; Akiyama, K.; Tero-Kubota, S. *Chem. Phys. Lett.* **1999**, *303*, 201.
(23) Nagano, Y.; Ikoma, T.; Akiyama, K.; Tero-Kubota, S. *J. Chem. Phys.* **2001**, *114*, 1775.
(24) Toyota, S.; Yamamori, T.; Asakura, M.; Oki, M. *Bull. Chem. Soc. Jpn.* **2000**, *73*, 205.
(25) Toyota, S.; Yamamori, T.; Makino, T.; Oki, M. *Bull. Chem. Soc. Jpn.* **2000**, *73*, 2591.
(26) Toyota, S.; Makino, T. *Tetrahedron Lett.* **2003**, *44*, 7775.
(27) Makino, T.; Toyota, S. *Bull. Chem. Soc. Jpn.* **2005**, *78*, 917.
(28) Toyota, S.; Yanagihara, T.; Yoshida, Y.; Goichi, M. *Bull. Chem. Soc. Jpn.* **2005**, *78*, 1351.
(29) Beeby, A.; Findlay, K. S.; Goeta, A. E.; Porres, L.; Rutter, S. R.; Thompson, A. L. *Photochem. Photobiol. Sci.* **2007**, *6*, 982.
(30) Yang, J.-S.; Yan, J.-L.; Hwang, C.-Y.; Chiou, S.-Y.; Liau, K.-L.; Gavin Tsai, H.-H.; Lee, G.-H.; Peng, S.-M. *J. Am. Chem. Soc.* **2006**, *128*, 14109.
(31) Yang, J.-S.; Yan, J.-L.; Lin, C.-K.; Chen, C.-Y.; Xie, Z.-Y.; Chen, C.-H. *Angew. Chem., Int. Ed.* **2009**, *48*, 9936.
(32) Miljanic, O. S.; Han, S.; Holmes, D.; Schaller, G. R.; Vollhardt, K. P. C. *Chem. Commun.* **2005**, 2606.
(33) Crisp, G. T.; Bubner, T. P. *Tetrahedron* **1997**, *53*, 11881.
(34) Shukla, R.; Brody, D. M.; Lindeman, S. V.; Rathore, R. *J. Org. Chem.* **2006**, *71*, 6124.
(35) Menning, S.; Krämer, M.; Coombs, B. A.; Rominger, F.; Beeby, A.; Dreuw, A.; Bunz, U. H. F. *J. Am. Chem. Soc.* **2013**, *135*, 2160.
(36) Stará, I. G.; Starý, I.; Kollárovič, A.; Teplý, F.; Šaman, D.; Fiedler, P. *Tetrahedron* **1998**, *54*, 11209.
(37) McFarland, S. A.; Finney, N. S. *J. Am. Chem. Soc.* **2002**, *124*, 1178.
(38) CCDC 918376 (**1**), 918377 (**2**), 970881 (**3**), 970882 (**4**), 970883 (**5**), 970884 (**6**), 970885 (**7**), 918378 (**8**), 918379 (**9**) contain the supplementary crystallographic data for this paper. These data can be obtained free of charge from The Cambridge Crystallographic Data Centre via www.ccdc.cam.ac.uk/data_request/cif.
(39) Torsion angles were determined by fitting a plane through each phenyl ring and measuring the angle of the planes.
(40) Dunning, T. H. *J. Chem. Phys.* **1989**, *90*, 1007.
(41) Grimme, S.; Antony, J.; Ehrlich, S.; Krieg, H. *J. Chem. Phys.* **2010**, *132*, 154104.
(42) Grimme, S.; Ehrlich, S.; Goerigk, L. *J. Comput. Chem.* **2011**, *32*, 1456.

(43) Sluch, M. I.; Godt, A.; Bunz, U. H. F.; Berg, M. A. *J. Am. Chem. Soc.* **2001**, *123*, 6447.
(44) Runge, E.; Gross, E. K. U. *Phys. Rev. Lett.* **1984**, *52*, 997.
(45) Casida, M. E. In *In Recent Advances in Density Functional Methods (Part I)*; Chong, D. P., Ed.; World Scientific: Singapore, 1995; Vol. *1*, p 155.
(46) Dreuw, A.; Head-Gordon, M. *Chem. Rev.* **2005**, *105*, 4009.
(47) Yanai, T.; Tew, D. P.; Handy, N. C. *Chem. Phys. Lett.* **2004**, *393*, 51.
(48) El-Sayed, M. A. *J. Chem. Phys.* **1963**, *38*, 2834.
(49) Fulmer, G. R.; Miller, A. J. M.; Sherden, N. H.; Gottlieb, H. E.; Nudelman, A.; Stoltz, B. M.; Bercaw, J. E.; Goldberg, K. I. *Organometallics* **2010**, *29*, 2176.
(50) Nakatani, K.; Takada, K.; Isoe, S. *J. Org. Chem.* **1995**, *60*, 2466.
(51) Dervan, P. B.; Jones, C. R. *J. Org. Chem.* **1979**, *44*, 2116.
(52) Nolis, P.; Virgili, A. *J. Org. Chem.* **2006**, *71*, 3267.
(53) Lowe, A. J.; Dyson, G. A.; Pfeffer, F. M. *Eur. J. Org. Chem.* **2008**, *2008*, 1559.